NASA Technical Memorandum 110352

Calculation of Three-Dimensional (3-D) Internal Flow by Means of the Velocity-Vorticity Formulation on a Staggered Grid

Paul M. Stremel

May 1995

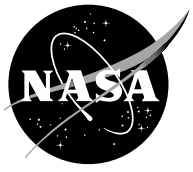

National Aeronautics and
Space Administration

NASA Technical Memorandum 110352

Calculation of Three-Dimensional (3-D) Internal Flow by Means of the Velocity-Vorticity Formulation on a Staggered Grid

Paul M. Stremel, Ames Research Center, Moffett Field, California

May 1995

National Aeronautics and
Space Administration

Ames Research Center
Moffett Field, CA 94035-1000

NOMENCLATURE

$\vec{a}_{1,2,3}$	unit vectors in transformed space
$h_{1,2,3}$	vector length in transformed space
l	reference length
n	nondimensional time index
r	radius
R_e	Reynolds number, U_∞ l/ν
t	time
u	velocity component in x-direction
$u_{1,2,3}$	transformed velocity component
v	velocity component in y-direction
w	velocity component in z-direction
x	Cartesian coordinate
y	Cartesian coordinate
z	Cartesian coordinate
θ	angular displacement
ν	kinematic viscosity
$\xi_{1,2,3}$	coordinate in transformed space
ω	vorticity
$\omega_{1,2,3}$	vorticity components in transformed space

Subscripts

$()_\infty$	value at upper plate

Superscripts

$( )'$	dimensional quantity
$\vec{( )}$	vector quantity
$( )^*$	quantity at first fractional step
$( )^{**}$	quantity at second fractional step
$( )^n$	quantity at nth time step
$( )^{n+1}$	quantity at (n + 1)th time step

CALCULATION OF THREE-DIMENSIONAL (3-D) INTERNAL FLOW BY MEANS OF THE VELOCITY-VORTICITY FORMULATION ON A STAGGERED GRID

Paul M. Stremel

Ames Research Center

SUMMARY

A method has been developed to accurately compute the viscous flow in three-dimensional (3-D) enclosures. This method is the 3-D extension of a two-dimensional (2-D) method developed for the calculation of flow over airfoils. The 2-D method has been tested extensively and has been shown to accurately reproduce experimental results. As in the 2-D method, the 3-D method provides for the non-iterative solution of the incompressible Navier–Stokes equations by means of a fully coupled implicit technique. The solution is calculated on a body fitted computational mesh incorporating a staggered grid methodology. In the staggered grid method, the three components of vorticity are defined at the centers of the computational cell sides, while the velocity components are defined as normal vectors at the centers of the computational cell faces. The staggered grid orientation provides for the accurate definition of the vorticity components at the vorticity locations, the divergence of vorticity at the mesh cell nodes and the conservation of mass at the mesh cell centers. The solution is obtained by utilizing a fractional step solution technique in the three coordinate directions. The boundary conditions for the vorticity and velocity are calculated implicitly as part of the solution. The method provides for the non-iterative solution of the flow field and satisfies the conservation of mass and divergence of vorticity to machine zero at each time step. To test the method, the calculation of simple driven cavity flows have been computed. The driven cavity flow is defined as the flow in an enclosure driven by a moving upper plate at the top of the enclosure. To demonstrate the ability of the method to predict the flow in arbitrary cavities, results will be shown for both cubic and curved cavities.

INTRODUCTION

The numerical prediction of vortex-dominated flow is paramount to the understanding of the flow about aircraft configurations. This is especially important to the design analysis of rotorcraft when considering download, the force exerted on the vehicle due to the rotor-wake interaction with the fuselage components. Download limits helicopter performance in hover and is a significant problem in the design of tilt-rotor configurations, where the lifting wing is immersed in the rotor wake. Because the download caused by the rotor wake severely limits the hover performance of tilt-rotor configurations, a method for accurately predicting tilt-rotor download would provide for the design of configurations with improved hover performance.

A two-dimensional (2-D) method has previously been developed to calculate the flow about bluff bodies, reference 1. Results have also been obtained for airfoils with and without a deflected flap at –90 deg incidence, reference 2. Additionally, the effect of Reynolds number and turbulence have been computed for the XV-15 wing airfoil with and without a deflected flap, reference 3. The results of reference 3 indicate that the flow field solution is highly Reynolds number and turbulence dependent. Excellent correlation between prediction and test were obtained when matching the test Reynolds number and incorporating the Baldwin/Barth turbulence model, reference 4. This correlation provides confidence in using the current method as a tool to further investigate the reduction of drag on airfoils at –90 deg incidence.

The validated 2-D computational method has also been applied to calculate the influence of upper- or lower- surface fences on airfoil aerodynamics, reference 5. In particular, the flow about an XV-15 airfoil with a 30 percent trailing edge flap deflected 60 deg at –90 deg incidence was considered. The flow is calculated for a Reynolds number of one million while modeling turbulent flow. The results of that investigation indicate that significant reductions in drag are obtained with the inclusion of fences. In particular, a 35 percent drag reduction, with respect to the basic airfoil value, was achieved for a lower-surface fence located at the airfoil leading edge.

The ability of the 2-D method to accurately compute the flow about a complex geometry normal to the free-stream flow and the direct extension of the method to 3-D analysis are the basis for this paper. In order to predict download, a method is required that can, not only, compute the flow about complex 3-D bodies, but also can accurately predict the wing-base pressure, which has been illusive. The 3-D extension of the 2-D analysis promises to be such a method.

Prior to solving the 3-D external flow problem a simpler problem is addressed to validate the governing equations and the solution technique. The flow in a driven cavity is considered to test the method. The development of the method is presented in the next section followed by the application of the method to the driven cavity problem.

PROBLEM FORMULATION

The flow field is modeled by the velocity/vorticity form of the unsteady, incompressible Navier–Stokes equations. The nondimensional governing equations in Cartesian coordinates are written for the continuity equation,

$$\vec{\nabla} \bullet \vec{u} = 0 \tag{1}$$

and for the vorticity transport equation,

$$\vec{\omega}_t + \vec{\nabla} \times \left(\vec{\omega} \times \vec{u} \right) = \nabla^2 \vec{\omega} / R_e \tag{2}$$

with $\nabla^2 = \partial^2( )/\partial \times^2 + \partial^2( )/\partial y^2 + \partial^2( )/\partial z^2$, where (x,y,z) are the Cartesian coordinates, R_e is the Reynolds number, and t is the time. The vorticity, ω, is defined by

$$\vec{\omega} = \vec{\nabla} \times \vec{u} \tag{3}$$

The nondimensional variables are written

$$x = x' / l, y = y' / l, z = z' / l$$
$$u = u' / U_\infty, v = v' / U_\infty, w = w' / U_\infty$$
$$\omega = \omega' / \left(U_\infty / l\right), t = t' / \left(l / U_\infty\right), R_e = U_\infty l / \nu$$

where

u, v, and w are the Cartesian components of the velocity, and

l = reference length

R_e = Reynolds number based on l

U_∞ = free-stream velocity

ν = kinematic viscosity

When the Cartesian equations are transformed into generalized-orthogonal-curvalinear coordinates, the governing equations become as follows (see ref. 6 for details).

For the continuity equation,

$$\vec{\nabla} \bullet \vec{u} = \frac{1}{h_1 h_2 h_3}\left[\frac{\partial\left(h_2 h_3 u_1\right)}{\partial \xi_1} + \frac{\partial\left(h_1 h_3 u_2\right)}{\partial \xi_2} + \frac{\partial\left(h_1 h_2 u_3\right)}{\partial \xi_3}\right] = 0 \tag{4}$$

and for the definition of vorticity,

$$\vec{\omega} = \left[\frac{1}{h_2 h_3}\left(\frac{\partial\left(h_3 u_3\right)}{\partial \xi_2} - \frac{\partial\left(h_2 u_2\right)}{\partial \xi_3}\right)\right]\vec{a}_1 + \left[\frac{1}{h_1 h_3}\left(\frac{\partial\left(h_1 u_1\right)}{\partial \xi_3} - \frac{\partial\left(h_3 u_3\right)}{\partial \xi_1}\right)\right]\vec{a}_2 + \left[\frac{1}{h_1 h_2}\left(\frac{\partial\left(h_2 u_2\right)}{\partial \xi_1} - \frac{\partial\left(h_1 u_1\right)}{\partial \xi_2}\right)\right]\vec{a}_3 \tag{5}$$

where (ξ_1,ξ_2,ξ_3) are the transformed coordinates, u_1, u_2, and u_3 are the orthogonal velocity components in the transformed coordinates, and h_1, h_2, and h_3 are the vector lengths,

$$h_1 = \left\{\left(\frac{\partial x}{\partial \xi_1}\right)^2 + \left(\frac{\partial y}{\partial \xi_1}\right)^2 + \left(\frac{\partial z}{\partial \xi_1}\right)^2\right\}^{\frac{1}{2}}$$

$$h_2 = \left\{ \left(\frac{\partial x}{\partial \xi_2} \right)^2 + \left(\frac{\partial y}{\partial \xi_2} \right)^2 + \left(\frac{\partial z}{\partial \xi_2} \right)^2 \right\}^{\frac{1}{2}}$$

$$h_3 = \left\{ \left(\frac{\partial x}{\partial \xi_3} \right)^2 + \left(\frac{\partial y}{\partial \xi_3} \right)^2 + \left(\frac{\partial z}{\partial \xi_3} \right)^2 \right\}^{\frac{1}{2}}$$

The vorticity transport equation, equation 2, can be rewritten as:

$$\vec{\omega}_t + \vec{u} \bullet \vec{\nabla} \vec{\omega} - \vec{\omega} \bullet \vec{\nabla} \vec{u} = \nabla^2 \vec{\omega} / R_e \tag{6}$$

This form offers some unique issues regarding the dot product on the left-hand side and the Laplacian operator on the right-hand side of the equation. Because both the gradient and the Laplacian operator act on a vector quantity, the dependence of the vector components and the unit vectors must be considered. The expression for $\vec{u} \bullet \vec{\nabla} \vec{\omega}$ becomes:

$$\begin{aligned}
&\vec{u} \bullet \nabla \vec{\omega} \\
&= \left[\vec{u} \bullet \nabla \omega_1 + \frac{\omega_2}{h_1 h_2} \left(u_1 \frac{\partial h_1}{\partial \xi_2} - u_2 \frac{\partial h_2}{\partial \xi_1} \right) + \frac{\omega_3}{h_1 h_3} \left(u_1 \frac{\partial h_1}{\partial \xi_3} - u_3 \frac{\partial h_3}{\partial \xi_1} \right) \right] \vec{a}_1 \\
&\quad + \left[\vec{u} \bullet \nabla \omega_2 + \frac{\omega_1}{h_1 h_2} \left(u_2 \frac{\partial h_2}{\partial \xi_1} - u_1 \frac{\partial h_1}{\partial \xi_2} \right) + \frac{\omega_3}{h_2 h_3} \left(u_2 \frac{\partial h_2}{\partial \xi_3} - u_3 \frac{\partial h_3}{\partial \xi_2} \right) \right] \vec{a}_2 \\
&\quad + \left[\vec{u} \bullet \nabla \omega_3 + \frac{\omega_1}{h_1 h_3} \left(u_3 \frac{\partial h_3}{\partial \xi_1} - u_1 \frac{\partial h_1}{\partial \xi_3} \right) + \frac{\omega_2}{h_2 h_3} \left(u_3 \frac{\partial h_3}{\partial \xi_2} - u_2 \frac{\partial h_2}{\partial \xi_3} \right) \right] \vec{a}_3
\end{aligned}$$

Where, $\nabla(\ ) = \left[\frac{1}{h_1} \frac{\partial(\ )}{\partial \xi_1} \vec{a}_1 + \frac{1}{h_2} \frac{\partial(\ )_1}{\partial \xi_2} \vec{a}_2 + \frac{1}{h_3} \frac{\partial(\ )}{\partial \xi_3} \vec{a}_3 \right]$. Details can be found in Appendix 1.

The expression for the Laplacian of the vorticity vector on the right-hand side of equation 6 is extremely long and can also be found in Appendix 1.

The boundary conditions for the transformed governing equations at the enclosure surface are calculated from the no-slip condition as

$$u_1 = u_2 = u_3 = 0 \tag{7}$$

except at the upper surface of the enclosure at which the velocity is specified. The surface vorticity is calculated from equation 5.

The flow is started impulsively. Therefore, at t = 0, the velocity on the upper surface of the enclosure is set to the prescribed boundary condition and the velocity everywhere inside the enclosure is set equal to zero. The vorticity on the upper surface of the enclosure is calculated from equation 5 and is set equal to zero everywhere else in the enclosure. The surface vorticity is calculated implicitly as part of the solution after the impulsive start. The computation is advanced until a desired time has been reached or until the flow has demonstrated stable periodic flow within the enclosure.

NUMERICAL METHOD

The solution is obtained by solving the finite-difference representations of the governing equations on a computational mesh. The grid is body-fitted to the interior of the 3-D enclosure.

In the staggered-grid method, the flow-field variables are not defined at the mesh nodes only. Rather, the components of vorticity are defined at the mid-points of the mesh cell sides, and the orthogonal flow-field velocity components are defined at the centers of the mesh cell faces. The vorticity and velocity components on the staggered grid are depicted in figure 1. The staggered-grid orientation of the variables provides for the conservation of vorticity at the mesh nodes and the solution of the continuity equation at the mesh cell centroids. The vorticity and flow-field velocities are calculated by a fully coupled implicit technique on the staggered mesh. The coupled method solves for the vorticity and velocity components by means of a block-tridiagonal inversion for fractional steps. A representation of the fractional step method is presented in Appendix 2. Each fractional step represents a computational sweep in one of the coordinate directions. These computational sweeps are depicted in figures 2–4.

In figure 2, the computational sweep for coordinate ξ_1 is shown. The governing equations for the vorticity and velocity components are selected to take into account the spatial derivatives in ξ_1. With this in mind, the conservation of vorticity is solved for ω_1. The vorticity components ω_2 and ω_3 are solved using the second and third components of the vorticity transport equation, equation 6. The continuity equation, equation 4, is solved for u_1, and the velocity components u_2 and u_3 are solved from the third and second components of vorticity, respectively, in equation 5. This allows for the ξ_1 derivatives of u_2 and u_3 to appear in the governing equation for each velocity component. Then for u_2,

$$\omega_3 = \frac{1}{h_1 h_2}\left(\frac{\partial(h_2 u_2)}{\partial \xi_1} - \frac{\partial(h_1 u_1)}{\partial \xi_2}\right)$$

and for u_3,

$$\omega_2 = \frac{1}{h_1 h_3}\left(\frac{\partial(h_1 u_1)}{\partial \xi_3} - \frac{\partial(h_3 u_3)}{\partial \xi_1}\right)$$

In figure 3, the computational sweep for coordinate ξ_2 is shown. The governing equations for the vorticity and velocity components are selected to take into account the spatial derivatives in ξ_2. Now, the conservation of vorticity is solved for ω_2. The vorticity components ω_1 and ω_3 are solved using the first and third components of the vorticity transport equation, equation 6. The continuity equation, equation 4, is solved for u_2, and the velocity components u_1 and u_3 are solved from the third and first components of vorticity, respectively, in equation 5. This allows for the ξ_2 derivatives of u_1 and u_3 to appear in the governing equation for each velocity component. Then for u_1,

$$\omega_3 = \frac{1}{h_1 h_2}\left(\frac{\partial(h_2 u_2)}{\partial \xi_1} - \frac{\partial(h_1 u_1)}{\partial \xi_2}\right)$$

and for u_3,

$$\omega_1 = \frac{1}{h_2 h_3}\left(\frac{\partial(h_3 u_3)}{\partial \xi_2} - \frac{\partial(h_2 u_2)}{\partial \xi_3}\right)$$

In figure 4, the computational sweep for coordinate ξ_3 is shown. The governing equations for the vorticity and velocity components are selected to take into account the spatial derivatives in ξ_3. Now, the conservation of vorticity is solved for ω_3. The vorticity components ω_1 and ω_2 are solved using the first and second components of the vorticity transport equation, equation 6. The continuity equation, equation 4, is solved for u_3, and the velocity components u_1 and u_2 are solved from the second and first components of vorticity, respectively, in equation 5. This allows for the ξ_2 derivatives of u_1 and u_3 to appear in the governing equation for each velocity component. Then for u_1,

$$\omega_2 = \frac{1}{h_1 h_3}\left(\frac{\partial(h_1 u_1)}{\partial \xi_3} - \frac{\partial(h_3 u_3)}{\partial \xi_1}\right)$$

and for u_2,

$$\omega_1 = \frac{1}{h_2 h_3}\left(\frac{\partial(h_3 u_3)}{\partial \xi_2} - \frac{\partial(h_2 u_2)}{\partial \xi_3}\right)$$

The boundary conditions are calculated implicitly as part of the solution. After the inversion of these block-tridiagonal systems, the solution for the present time-step is obtained. The solution is not iterated and the continuity equation is satisfied to machine zero. The solution is then advanced by updating the flow-field variables and solving the flow for the next time-step. The solution is terminated at a desired time or after sufficient time has elapsed for demonstration of the flow-field periodicity.

RESULTS

In order to test the method, the solution to the driven cavity problem was computed. All solutions were computed for a Reynolds number of 100. This geometry was considered to test the methodology and not to analyze the flow of driven cavities. The current formulation provides for the solution of 3-D, incompressible flow for arbitrary geometries and not constrained to Cartesian coordinates. The driven cavity problem is applied for a cubic cavity with constant coordinate spacing and with a cosine spacing, which clusters the grid lines at the boundaries. The results are compared to those computed in reference 8 for a cubic cavity of constant grid spacing in Cartesian coordinates. A curved cavity is also considered, again with a constant coordinate spacing and a cosine spacing for the grid coordinates. The cross-flow geometry for the four grids considered are shown in figures 5–8. The 3-D grids are constructed by stacking the cross-flow geometry. The velocity of the upper surface of the cavity is specified and held constant. The solution is started impulsively from rest and is continued until a steady solution is reached.

Cubic Cavity – Constant Grid Spacing

The driven cavity flow for the geometry of figure 5 is computed. For this solution, x is synonymous with ξ_1, y with ξ_2, and z with ξ_3. The upper plate, the x-y plane at maximum z, is held at a constant velocity, $U_\infty = 1.0$. The vorticity contours at the mid-plane locations are shown in figure 9. The ξ_1 vorticity, shown in figure 9(a), demonstrates the symmetric nature of the flow field with opposite vortices at the center of the plane and flow up the walls at y = 0 and y = 1.0. Additionally, secondary vortices form on the bottom of the cavity and on the upper plate. The ξ_2 vorticity, shown in figure 9(b), develops similar to the vorticity for a 2-D solution of the driven cavity problem. The ξ_3 vorticity, shown in figure 9(c), demonstrates the symmetric nature of the cavity flow with secondary vortices on the upstream wall. The vorticity contours of figure 9 are similar to the vorticity contours presented in reference 8.

Cubic Cavity – Cosine Grid Spacing

The driven cavity flow for the geometry of figure 6 is computed. This is similar to the previous solution. However with the increased grid resolution at the wall, additional flow features in the form of secondary vortices are resolved. Here again, x is synonymous with ξ_1, y with ξ_2, and z with ξ_3 and the upper plate is held at a constant velocity, $U_\infty = 1.0$. The vorticity contours at the mid-plane locations are shown in figure 10. The ξ_1 vorticity, shown in figure 10(a), demonstrates the symmetric nature of the flow field with opposite vortices at the center of the plane and flow up the walls at y = 0 and y = 1.0 and the enhanced flow features, such as, secondary vortices on the bottom of the cavity and on the upper plate. The ξ_2 vorticity, shown in figure 10(b), develops similar to the vorticity in the 2-D solution of the driven cavity problem and the previous vorticity shown in figure 9(b). Vortices in the lower corners of the cavity are clearly predicted. The ξ_3 vorticity, shown in figure 10(c), demonstrates the symmetric nature of the cavity flow with secondary vortices on the upstream and downstream wall. The vorticity contours in figure 10 are similar to those of figure 9 and the vorticity contours presented in reference 8.

Curved Cavity – Constant Grid Spacing

The driven cavity flow for the geometry of figure 7 is computed. For this solution, r, or radius, is synonymous with ξ_1, y with ξ_2, and θ with ξ_3. The upper plate, the x-y plane at maximum z, is held at a constant velocity, $U_\infty = 1.0$, see figure 7. The vorticity contours at the mid-plane locations are shown in figure 11. The ξ_1 vorticity, shown in figure 11(a), again demonstrates the symmetric nature of the flow field with opposite vortices at the center of the plane and flow up the walls at y = 0 and y = 1.0. Secondary vortices shown for the cubic cavity, figure 9(a), are not present here owing to the curvature and increased height of the cavity, both of which tend to stagnate the flow at the bottom of the cavity. The ξ_2 vorticity, shown in figure 11(b), develops similarly to the vorticity shown in figure 9(b) for the cubic cavity. However, the vorticity develops further down the downstream wall due to the curvature of the cavity. The ξ_3 vorticity, shown in figure 11(c), demonstrates the symmetric nature of the cavity flow with secondary vortices on the upstream wall.

Curved Cavity – Cosine Grid Spacing

The driven cavity flow for the geometry of figure 8 is computed. Here r, or radius, is synonymous with ξ_1, y with ξ_2, and θ with ξ_3. The upper plate, the x-y plane at maximum z, is held at a constant velocity, $U_\infty = 1.0$. The vorticity contours at the mid-plane locations are shown in figure 12. The ξ_1 vorticity, shown in figure 12(a), again demonstrates the symmetric nature of the flow field with opposite vortices at the center of the plane and flow up the walls at y = 0 and y = 1.0. The secondary vortex structure shown on the upper plate is better defined, when compared to that of the constant grid spacing, figure 11(a). The ξ_2 vorticity, shown in figure 12(b), develops similar to the vorticity shown in figure 11(b). However, corner vortices can be seen in the bottom of the cavity and increased rollup of the primary vortex in the center of the cavity. The ξ_3 vorticity, shown in figure 12(c), demonstrates the symmetric nature of the cavity flow with secondary vortices on the upstream and downstream walls.

CONCLUSIONS

A method has been developed to calculate accurately the viscous flow in 3-D enclosures. The method provides for the non-iterative solution of the incompressible Navier–Stokes equations by means of a fully coupled implicit technique. To demonstrate the method, the calculation of simple driven cavity flows has been considered. The driven cavity flow is defined as the flow in an enclosure driven by a moving upper plate at the top of the enclosure. The intent was not to present a study of cavity flows, but to determine the ability of the method to predict arbitrary internal 3-D flow. Therefore, results were shown for both cubic and curved cavities with constant and varying mesh spacing.

The predicted vorticity contours for a cubic cavity with constant mesh spacing were in close agreement with the contours shown in reference 8. The method predicted the emergence of the primary vortices, as well as, secondary vortices. Similar results were shown for a cubic cavity with a

cosine spacing for the grid points. The cosine spacing of the grid points concentrates the mesh points near the boundaries. With the cosine spacing, the primary and secondary vortices were enhanced.

The predicted vorticity contours for a curved cavity with constant mesh spacing were similar to those for the cubic cavity, and were again enhanced when the solution was computed on a curved cavity with a cosine distribution for the grid points.

The comparison of the present results with other computations for the cubic cavity flow and the comparison of the cubic cavity flow with the curved cavity flow provide credibility to the methodology. Considerable work is required to extend the method to external flows, to incorporate turbulence models and to apply the method to realistic problems.

APPENDIX 1

This Appendix presents the development of the dot-product, divergence, and LaPlacian operator of a vector quantity and are integral to the development of the generalized governing equations in three-dimensional (3-D) space.

The expressions in this Appendix are written for a general vector quantity,

$$\vec{F} = F_1\vec{a}_1 + +F_2\vec{a}_2 + F_3\vec{a}_3$$

The dot product of a vector with the gradient of another vector is written,

$$\vec{n} \bullet \nabla\vec{F} = \vec{n} \bullet \nabla\left(F_1\vec{a}_1 + F_1\vec{a}_2 + F_3\vec{a}_3\right)$$

or,

$$\vec{n} \bullet \nabla\vec{F} = \vec{n} \bullet \nabla F_1\vec{a}_1 + \vec{n} \bullet \nabla F_2\vec{a}_2 + \vec{n} \bullet \nabla F_3\vec{a}_3 + F_1\left(\vec{n} \bullet \nabla\vec{a}_1\right) + F_2\left(\vec{n} \bullet \nabla\vec{a}_2\right) + F_3\left(\vec{n} \bullet \nabla\vec{a}_3\right)$$

The general expressions for the dot product and the gradient are, respectively,

$$\nabla \bullet \vec{F} = \frac{1}{h_1h_2h_3}\left[\frac{\partial\left(h_2h_3F_1\right)}{\partial\xi_1} + \frac{\partial\left(h_1h_3F_2\right)}{\partial\xi_2} + \frac{\partial\left(h_1h_2F_3\right)}{\partial\xi_3}\right]$$

and,

$$\nabla F_1 = \left[\frac{1}{h_1}\frac{\partial F_1}{\partial\xi_1}\vec{a}_1 + \frac{1}{h_2}\frac{\partial F_1}{\partial\xi_2}\vec{a}_2 + \frac{1}{h_3}\frac{\partial F_1}{\partial\xi_3}\vec{a}_3\right]$$

Using the following expressions for the derivatives of the unit vectors,

$$\frac{\partial\vec{a}_1}{\partial\xi_1} = -\frac{1}{h_2}\frac{\partial h_1}{\partial\xi_2}\vec{a}_2 - \frac{1}{h_3}\frac{\partial h_1}{\partial\xi_3}\vec{a}_3, \frac{\partial\vec{a}_1}{\partial\xi_2} = \frac{1}{h_1}\frac{\partial h_2}{\partial\xi_1}\vec{a}_2, \frac{\partial\vec{a}_1}{\partial\xi_3} = \frac{1}{h_1}\frac{\partial h_3}{\partial\xi_1}\vec{a}_3$$

$$\frac{\partial\vec{a}_2}{\partial\xi_1} = \frac{1}{h_2}\frac{\partial h_1}{\partial\xi_2}\vec{a}_1, \frac{\partial\vec{a}_2}{\partial\xi_2} = -\frac{1}{h_1}\frac{\partial h_2}{\partial\xi_1}\vec{a}_1 - \frac{1}{h_3}\frac{\partial h_2}{\partial\xi_3}\vec{a}_3, \frac{\partial\vec{a}_2}{\partial\xi_3} = \frac{1}{h_2}\frac{\partial h_3}{\partial\xi_2}\vec{a}_3$$

$$\frac{\partial\vec{a}_3}{\partial\xi_1} = \frac{1}{h_3}\frac{\partial h_1}{\partial\xi_3}\vec{a}_1, \frac{\partial\vec{a}_3}{\partial\xi_2} = \frac{1}{h_3}\frac{\partial h_2}{\partial\xi_3}\vec{a}_2, \frac{\partial\vec{a}_3}{\partial\xi_3} = -\frac{1}{h_1}\frac{\partial h_3}{\partial\xi_1}\vec{a}_1 - \frac{1}{h_2}\frac{\partial h_3}{\partial\xi_2}\vec{a}_2$$

the dot product of the unit vectors become,

$$\vec{n} \bullet \nabla \vec{a}_1 = \left[\frac{n_1}{h_1} \frac{\partial \vec{a}_1}{\partial \xi_1} + \frac{n_2}{h_2} \frac{\partial \vec{a}_1}{\partial \xi_2} + \frac{n_3}{h_3} \frac{\partial \vec{a}_1}{\partial \xi_3} \right]$$

or,

$$\vec{n} \bullet \nabla a_1 = \left[\frac{n_1}{h_1} \left(-\frac{1}{h_2} \frac{\partial h_1}{\partial \xi_2} \vec{a}_2 - \frac{1}{h_3} \frac{\partial h_1}{\partial \xi_3} \vec{a}_3 \right) + \frac{n_2}{h_2} \frac{1}{h_1} \frac{\partial h_2}{\partial \xi_1} \vec{a}_2 + \frac{n_3}{h_3} \frac{1}{h_1} \frac{\partial h_3}{\partial \xi_1} \vec{a}_3 \right]$$

and,

$$\vec{n} \bullet \nabla \vec{a}_2 = \left[\frac{n_1}{h_1} \frac{\partial \vec{a}_2}{\partial \xi_1} + \frac{n_2}{h_2} \frac{\partial \vec{a}_2}{\partial \xi_2} + \frac{n_3}{h_3} \frac{\partial \vec{a}_2}{\partial \xi_3} \right]$$

or,

$$\vec{n} \bullet \nabla \vec{a}_2 = \left[\frac{n_1}{h_1} \frac{1}{h_2} \frac{\partial h_1}{\partial \xi_2} \vec{a}_1 + \frac{n_2}{h_2} \left(-\frac{1}{h_1} \frac{\partial h_2}{\partial \xi_1} \vec{a}_1 - \frac{1}{h_3} \frac{\partial h_2}{\partial \xi_3} \vec{a}_3 \right) + \frac{n_3}{h_3} \frac{1}{h_2} \frac{\partial h_3}{\partial \xi_2} \vec{a}_3 \right]$$

and,

$$\vec{n} \bullet \nabla \vec{a}_3 = \left[\frac{n_1}{h_1} \frac{\partial \vec{a}_3}{\partial \xi_1} + \frac{n_2}{h_2} \frac{\partial \vec{a}_3}{\partial \xi_2} + \frac{n_3}{h_3} \frac{\partial \vec{a}_3}{\partial \xi_3} \right]$$

or,

$$\vec{n} \bullet \nabla \vec{a}_3 = \left[\frac{n_1}{h_1} \frac{1}{h_3} \frac{\partial h_1}{\partial \xi_3} \vec{a}_1 + \frac{n_2}{h_2} \frac{1}{h_3} \frac{\partial h_2}{\partial \xi_3} \vec{a}_2 + \frac{n_3}{h_3} \left(-\frac{1}{h_1} \frac{\partial h_3}{\partial \xi_1} \vec{a}_1 - \frac{1}{h_2} \frac{\partial h_3}{\partial \xi_2} \vec{a}_2 \right) \right]$$

Then the dot product becomes,

$$\begin{aligned}
&\vec{n}\bullet\nabla\vec{F}\\
&=\vec{n}\bullet\nabla F_1\vec{a}_1+\vec{n}\bullet\nabla F_2\vec{a}_2+\vec{n}\bullet\nabla F_3\vec{a}_3\\
&+F_1\left[\frac{n_1}{h_1}\left(-\frac{1}{h_2}\frac{\partial h_1}{\partial\xi_2}\vec{a}_2-\frac{1}{h_3}\frac{\partial h_1}{\partial\xi_3}\vec{a}_3\right)+\frac{n_2}{h_2}\frac{1}{h_1}\frac{\partial h_2}{\partial\xi_1}\vec{a}_2+\frac{n_3}{h_3}\frac{1}{h_1}\frac{\partial h_3}{\partial\xi_1}\vec{a}_3\right]\\
&+F_2\left[\frac{n_1}{h_1}\frac{1}{h_2}\frac{\partial h_1}{\partial\xi_2}\vec{a}_1+\frac{n_2}{h_2}\left(-\frac{1}{h_1}\frac{\partial h_2}{\partial\xi_1}\vec{a}_1-\frac{1}{h_3}\frac{\partial h_2}{\partial\xi_3}\vec{a}_3\right)+\frac{n_3}{h_3}\frac{1}{h_2}\frac{\partial h_3}{\partial\xi_2}\vec{a}_3\right]\\
&+F_3\left[\frac{n_1}{h_1}\frac{1}{h_3}\frac{\partial h_1}{\partial\xi_3}\vec{a}_1+\frac{n_2}{h_2}\frac{1}{h_3}\frac{\partial h_2}{\partial\xi_3}\vec{a}_2+\frac{n_3}{h_3}\left(-\frac{1}{h_1}\frac{\partial h_3}{\partial\xi_1}\vec{a}_1-\frac{1}{h_2}\frac{\partial h_3}{\partial\xi_2}\vec{a}_2\right)\right]
\end{aligned}$$

or,

$$\begin{aligned}
&\vec{n}\bullet\nabla\vec{F}\\
&=\left[\vec{n}\bullet\nabla F_1+\frac{F_2}{h_1h_2}\left(n_1\frac{\partial h_1}{\partial\xi_2}-n_2\frac{\partial h_2}{\partial\xi_1}\right)+\frac{F_3}{h_1h_3}\left(n_1\frac{\partial h_1}{\partial\xi_3}-n_3\frac{\partial h_3}{\partial\xi_1}\right)\right]\vec{a}_1\\
&+\left[\vec{n}\bullet\nabla F_2+\frac{F_1}{h_1h_2}\left(n_2\frac{\partial h_2}{\partial\xi_1}-n_1\frac{\partial h_1}{\partial\xi_2}\right)+\frac{F_3}{h_2h_3}\left(n_2\frac{\partial h_2}{\partial\xi_3}-n_3\frac{\partial h_3}{\partial\xi_2}\right)\right]\vec{a}_2\\
&+\left[\vec{n}\bullet\nabla F_3+\frac{F_1}{h_1h_3}\left(n_3\frac{\partial h_3}{\partial\xi_1}-n_1\frac{\partial h_1}{\partial\xi_3}\right)+\frac{F_2}{h_2h_3}\left(n_3\frac{\partial h_3}{\partial\xi_2}-n_2\frac{\partial h_2}{\partial\xi_3}\right)\right]\vec{a}_3
\end{aligned}$$

The Laplacian of a vector is as follows.

The Laplacian of a scalar is written,

$$\nabla^2(\ )=\frac{1}{h_1h_2h_3}\left[\frac{\partial}{\partial\xi_1}\left(\frac{h_2h_3}{h_1}\frac{\partial(\ )}{\partial\xi_1}\right)+\frac{\partial}{\partial\xi_2}\left(\frac{h_1h_3}{h_2}\frac{\partial(\ )}{\partial\xi_2}\right)+\frac{\partial}{\partial\xi_1}\left(\frac{h_1h_2}{h_3}\frac{\partial(\ )}{\partial\xi_3}\right)\right]$$

For which the Laplacian for a vector quantity is written,

$$\nabla^2\vec{F}$$
$$= \frac{1}{h_1h_2h_3}\left[\frac{\partial}{\partial\xi_1}\left(\frac{h_2h_3}{h_1}\left(\vec{a}_1\frac{\partial F_1}{\partial\xi_1}+F_1\frac{\partial\vec{a}_1}{\partial\xi_1}+\vec{a}_2\frac{\partial F_2}{\partial\xi_1}+F_2\frac{\partial\vec{a}_2}{\partial\xi_1}+\vec{a}_3\frac{\partial F_3}{\partial\xi_1}+F_3\frac{\partial\vec{a}_3}{\partial\xi_1}\right)\right)\right]$$
$$+\frac{1}{h_1h_2h_3}\left[\frac{\partial}{\partial\xi_2}\left(\frac{h_1h_3}{h_2}\left(\vec{a}_1\frac{\partial F_1}{\partial\xi_2}+F_1\frac{\partial\vec{a}_1}{\partial\xi_2}+\vec{a}_2\frac{\partial F_2}{\partial\xi_2}+F_2\frac{\partial\vec{a}_2}{\partial\xi_2}+\vec{a}_3\frac{\partial F_3}{\partial\xi_2}+F_3\frac{\partial\vec{a}_3}{\partial\xi_2}\right)\right)\right]$$
$$+\frac{1}{h_1h_2h_3}\left[\frac{\partial}{\partial\xi_1}\left(\frac{h_1h_2}{h_3}\left(\vec{a}_1\frac{\partial F_1}{\partial\xi_3}+F_1\frac{\partial\vec{a}_1}{\partial\xi_3}+\vec{a}_2\frac{\partial F_2}{\partial\xi_3}+F_2\frac{\partial\vec{a}_2}{\partial\xi_3}+\vec{a}_3\frac{\partial F_3}{\partial\xi_3}+F_3\frac{\partial\vec{a}_3}{\partial\xi_3}\right)\right)\right]$$

After evaluation of the above terms using the product rule, incorporating the derivatives of the unit vectors presented above and considerable rearranging, the Laplacian of a vector quantity is written,

$$\nabla^2\vec{F}$$
$$= \frac{1}{h_1h_2h_3}\left[\begin{array}{l}\frac{\partial}{\partial\xi_1}\left(\frac{h_2h_3}{h_1}\frac{\partial F_1}{\partial\xi_1}\right)+\frac{\partial}{\partial\xi_2}\left(\frac{h_1h_3}{h_2}\frac{\partial F_1}{\partial\xi_2}\right)+\frac{\partial}{\partial\xi_3}\left(\frac{h_1h_2}{h_3}\frac{\partial F_1}{\partial\xi_3}\right)\\ -\frac{h_2}{h_1h_3}F_1\left(\frac{\partial h_3}{\partial\xi_1}\right)^2-\frac{h_3}{h_1h_2}F_1\left(\frac{\partial h_2}{\partial\xi_1}\right)^2-\frac{h_3}{h_1h_2}F_1\left(\frac{\partial h_1}{\partial\xi_2}\right)^2-\frac{h_2}{h_1h_3}F_1\left(\frac{\partial h_1}{\partial\xi_3}\right)^2\end{array}\right]\vec{a}_1$$
$$+\frac{1}{h_1h_2h_3}\left[2\frac{h_3}{h_1}\frac{\partial h_1}{\partial\xi_2}\frac{\partial F_2}{\partial\xi_1}+F_2\frac{\partial}{\partial\xi_1}\left(\frac{h_3}{h_1}\frac{\partial h_1}{\partial\xi_2}\right)\right]\vec{a}_1$$
$$+\frac{1}{h_1h_2h_3}\left[2\frac{h_2}{h_1}\frac{\partial h_1}{\partial\xi_3}\frac{\partial F_3}{\partial\xi_1}+F_3\frac{\partial}{\partial\xi_1}\left(\frac{h_2}{h_1}\frac{\partial h_1}{\partial\xi_3}\right)\right]\vec{a}_1$$
$$+\frac{1}{h_1h_2h_3}\left[-2\frac{h_3}{h_2}\frac{\partial h_2}{\partial\xi_1}\frac{\partial F_2}{\partial\xi_2}-F_2\frac{\partial}{\partial\xi_2}\left(\frac{h_3}{h_2}\frac{\partial h_2}{\partial\xi_1}\right)\right]\vec{a}_1$$
$$-\frac{1}{h_1h_2h_3}\left[\frac{1}{h_3}F_2\left(\frac{\partial h_3}{\partial\xi_2}\frac{\partial h_3}{\partial\xi_1}\right)+\frac{1}{h_2}F_3\left(\frac{\partial h_2}{\partial\xi_3}\frac{\partial h_2}{\partial\xi_1}\right)\right]\vec{a}_1$$
$$+\frac{1}{h_1h_2h_3}\left[-2\frac{h_2}{h_3}\frac{\partial h_3}{\partial\xi_1}\frac{\partial F_3}{\partial\xi_3}-F_3\frac{\partial}{\partial\xi_3}\left(\frac{h_2}{h_3}\frac{\partial h_3}{\partial\xi_1}\right)\right]\vec{a}_1$$

$$+\frac{1}{h_1h_2h_3}\left[\begin{array}{l}\frac{\partial}{\partial\xi_1}\left(\frac{h_2h_3}{h_1}\frac{\partial F_2}{\partial\xi_1}\right)+\frac{\partial}{\partial\xi_2}\left(\frac{h_1h_3}{h_2}\frac{\partial F_2}{\partial\xi_2}\right)+\frac{\partial}{\partial\xi_3}\left(\frac{h_1h_2}{h_3}\frac{\partial F_2}{\partial\xi_3}\right)\\ -\frac{h_1}{h_2h_3}F_2\left(\frac{\partial h_3}{\partial\xi_2}\right)^2-\frac{h_3}{h_1h_2}F_2\left(\frac{\partial h_2}{\partial\xi_1}\right)^2-\frac{h_1}{h_2h_3}F_2\left(\frac{\partial h_2}{\partial\xi_3}\right)^2-\frac{h_3}{h_1h_2}F_2\left(\frac{\partial h_1}{\partial\xi_2}\right)^2\end{array}\right]\vec{a}_2$$

$$+\frac{1}{h_1h_2h_3}\left[-2\frac{h_3}{h_1}\frac{\partial h_1}{\partial\xi_2}\frac{\partial F_1}{\partial\xi_1}-F_1\frac{\partial}{\partial\xi_1}\left(\frac{h_3}{h_1}\frac{\partial h_1}{\partial\xi_2}\right)\right]\vec{a}_2$$

$$+\frac{1}{h_1h_2h_3}\left[2\frac{h_3}{h_2}\frac{\partial h_2}{\partial\xi_1}\frac{\partial F_1}{\partial\xi_2}+F_1\frac{\partial}{\partial\xi_2}\left(\frac{h_3}{h_2}\frac{\partial h_2}{\partial\xi_1}\right)\right]\vec{a}_2$$

$$+\frac{1}{h_1h_2h_3}\left[2\frac{h_1}{h_2}\frac{\partial h_2}{\partial\xi_3}\frac{\partial F_3}{\partial\xi_2}+F_3\frac{\partial}{\partial\xi_2}\left(\frac{h_1}{h_2}\frac{\partial h_2}{\partial\xi_3}\right)\right]\vec{a}_2$$

$$-\frac{1}{h_1h_2h_3}\left[\frac{1}{h_3}F_1\left(\frac{\partial h_3}{\partial\xi_1}\frac{\partial h_3}{\partial\xi_2}\right)+\frac{1}{h_1}F_3\left(\frac{\partial h_1}{\partial\xi_3}\frac{\partial h_1}{\partial\xi_2}\right)\right]\vec{a}_2$$

$$+\frac{1}{h_1h_2h_3}\left[-2\frac{h_1}{h_3}\frac{\partial h_3}{\partial\xi_2}\frac{\partial F_3}{\partial\xi_3}-F_3\frac{\partial}{\partial\xi_3}\left(\frac{h_1}{h_3}\frac{\partial h_3}{\partial\xi_2}\right)\right]\vec{a}_2$$

$$+\frac{1}{h_1h_2h_3}\left[\begin{array}{l}\frac{\partial}{\partial\xi_1}\left(\frac{h_2h_3}{h_1}\frac{\partial F_3}{\partial\xi_1}\right)+\frac{\partial}{\partial\xi_2}\left(\frac{h_1h_3}{h_2}\frac{\partial F_3}{\partial\xi_2}\right)+\frac{\partial}{\partial\xi_3}\left(\frac{h_1h_2}{h_3}\frac{\partial F_3}{\partial\xi_3}\right)\\ -\frac{h_2}{h_1h_3}F_3\left(\frac{\partial h_3}{\partial\xi_1}\right)^2-\frac{h_1}{h_2h_3}F_3\left(\frac{\partial h_3}{\partial\xi_2}\right)^2-\frac{h_1}{h_2h_3}F_3\left(\frac{\partial h_2}{\partial\xi_3}\right)^2-\frac{h_2}{h_1h_3}F_3\left(\frac{\partial h_1}{\partial\xi_3}\right)^2\end{array}\right]\vec{a}_3$$

$$+\frac{1}{h_1h_2h_3}\left[-2\frac{h_2}{h_1}\frac{\partial h_1}{\partial\xi_3}\frac{\partial F_1}{\partial\xi_1}-F_1\frac{\partial}{\partial\xi_1}\left(\frac{h_2}{h_1}\frac{\partial h_1}{\partial\xi_3}\right)\right]\vec{a}_3$$

$$-\frac{1}{h_1h_2h_3}\left[\frac{1}{h_2}F_1\left(\frac{\partial h_2}{\partial\xi_1}\frac{\partial h_2}{\partial\xi_3}\right)+\frac{1}{h_1}F_2\left(\frac{\partial h_1}{\partial\xi_2}\frac{\partial h_1}{\partial\xi_3}\right)\right]\vec{a}_3$$

$$+\frac{1}{h_1h_2h_3}\left[-2\frac{h_1}{h_2}\frac{\partial h_2}{\partial\xi_3}\frac{\partial F_2}{\partial\xi_2}-F_2\left(\frac{\partial}{\partial\xi_2}\left(\frac{h_1}{h_2}\frac{\partial h_2}{\partial\xi_3}\right)\right)\right]\vec{a}_3$$

$$+\frac{1}{h_1 h_2 h_3}\left[2\frac{h_2}{h_3}\frac{\partial h_3}{\partial \xi_1}\frac{\partial F_1}{\partial \xi_3}+F_1\left(\frac{\partial}{\partial \xi_3}\left(\frac{h_2}{h_3}\frac{\partial h_3}{\partial \xi_1}\right)\right)\right]\vec{a}_3$$

$$+\frac{1}{h_1 h_2 h_3}\left[2\frac{h_1}{h_3}\frac{\partial h_3}{\partial \xi_2}\frac{\partial F_2}{\partial \xi_3}+F_2\frac{\partial}{\partial \xi_3}\left(\frac{h_1}{h_3}\frac{\partial h_3}{\partial \xi_2}\right)\right]\vec{a}_3$$

APPENDIX 2

This Appendix presents the development of the fractional-step method of reference 7 for three-dimensions. Consider the Cartesian form of the vorticity transport equation in three dimensions, without considering the vortex-stretching terms. The equation is written,

$$\frac{\partial \omega}{\partial t}+\frac{\partial (u\omega)}{\partial x}+\frac{\partial (v\omega)}{\partial y}+\frac{\partial (w\omega)}{\partial z}=\frac{1}{Re}\left(\frac{\partial^2 \omega}{\partial x^2}+\frac{\partial^2 \omega}{\partial y^2}+\frac{\partial^2 \omega}{\partial z^2}\right)$$

The fractional step method is written , for the three fractional steps, as

for the x-coordinate step,

$$\frac{\omega^{*}-\omega^{n}}{\Delta t}+\frac{1}{2}\left(\frac{\partial (u\omega)^{*}}{\partial x}+\frac{\partial (u\omega)^{n}}{\partial x}\right)+\frac{\partial (v\omega)^{n}}{\partial y}+\frac{\partial (w\omega)^{n}}{\partial z}=\frac{1}{Re}\left(\frac{1}{2}\left(\frac{\partial^2 \omega^{*}}{\partial x^2}+\frac{\partial^2 \omega^{n}}{\partial x^2}\right)+\frac{\partial^2 \omega^{n}}{\partial y^2}+\frac{\partial^2 \omega^{n}}{\partial z^2}\right)$$

for the y-coordinate step,

$$\frac{\omega^{**}-\omega^{n}}{\Delta t}+\frac{1}{2}\left(\frac{\partial (u\omega)^{*}}{\partial x}+\frac{\partial (u\omega)^{n}}{\partial x}\right)+\frac{1}{2}\left(\frac{\partial (v\omega)^{**}}{\partial y}+\frac{\partial (v\omega)^{n}}{\partial y}\right)+\frac{\partial (w\omega)^{n}}{\partial z}=$$

$$\frac{1}{Re}\left(\frac{1}{2}\left(\frac{\partial^2 \omega^{*}}{\partial x^2}+\frac{\partial^2 \omega^{n}}{\partial x^2}\right)+\frac{1}{2}\left(\frac{\partial^2 \omega^{**}}{\partial y^2}+\frac{\partial^2 \omega^{n}}{\partial y^2}\right)+\frac{\partial^2 \omega^{n}}{\partial z^2}\right)$$

and for the z-coordinate step,

$$\frac{\omega^{n+1}-\omega^{n}}{\Delta t}+\frac{1}{2}\left(\frac{\partial (u\omega)^{*}}{\partial x}+\frac{\partial (u\omega)^{n}}{\partial x}\right)+\frac{1}{2}\left(\frac{\partial (v\omega)^{**}}{\partial y}+\frac{\partial (v\omega)^{n}}{\partial y}\right)+\frac{1}{2}\left(\frac{\partial (w\omega)^{n+1}}{\partial z}+\frac{\partial (ww)^{n}}{\partial z}\right)=$$

$$\frac{1}{Re}\left(\frac{1}{2}\left(\frac{\partial^2 \omega^{*}}{\partial x^2}+\frac{\partial^2 \omega^{n}}{\partial x^2}\right)+\frac{1}{2}\left(\frac{\partial^2 \omega^{**}}{\partial y^2}+\frac{\partial^2 \omega^{n}}{\partial y^2}\right)+\frac{1}{2}\left(\frac{\partial^2 \omega^{n+1}}{\partial z^2}+\frac{\partial^2 \omega^{n}}{\partial z^2}\right)\right)$$

Then

$$2\frac{\left(\omega^{*}-\omega^{n}\right)}{\Delta t}+\left(\frac{\partial (u\omega)^{*}}{\partial x}+\frac{\partial (u\omega)^{n}}{\partial x}\right)+2\frac{\partial (v\omega)^{n}}{\partial y}+2\frac{\partial (w\omega)^{n}}{\partial z}$$

$$=\frac{1}{Re}\left(\left(\frac{\partial^2 \omega^{*}}{\partial x^2}+\frac{\partial^2 \omega^{n}}{\partial x^2}\right)+2\frac{\partial^2 \omega^{n}}{\partial y^2}+2\frac{\partial^2 \omega^{n}}{\partial z^2}\right)\left(\omega^{**}-\omega^{*}\right)$$

yields,

$$2\frac{\left(\omega^{**}-\omega^{*}\right)}{\Delta t}+\left(\frac{\partial(v\omega)^{**}}{\partial y}-\frac{\partial(v\omega)^{n}}{\partial y}\right)=\frac{1}{Re}\left(\frac{\partial^{2}\omega^{**}}{\partial y^{2}}-\frac{\partial^{2}\omega^{n}}{\partial y^{2}}\right)\left(\omega^{n+1}-\omega^{**}\right)$$

yields,

$$2\frac{\left(\omega^{n+1}-\omega^{**}\right)}{\Delta t}+\left(\frac{\partial(w\omega)^{n+1}}{\partial z}-\frac{\partial(ww)^{n}}{\partial z}\right)=\frac{1}{Re}\left(\frac{\partial^{2}\omega^{n+1}}{\partial z^{2}}-\frac{\partial^{2}\omega^{n}}{\partial z^{2}}\right)$$

REFERENCES

1. Stremel, P. M.: Calculation of Flow about Two-Dimensional Bodies by Means of the Velocity-Vorticity Formulation on a Staggered Grid. AIAA Paper 91-0600, Reno, Nev., 1991.

2. Stremel, P. M.: Calculation of Unsteady Airfoil Loads with and without Flap Deflection at –90 Degrees Incidence. AIAA Paper 91-3336, Baltimore, Md., 1991.

3. Stremel P. M: The Effect of Reynolds Number and Turbulence on Airfoil Aerodynamics at –90 Degrees Incidence. AIAA Paper 93-0206, AIAA 31st Aerospace Sciences Meeting, Reno, Nev., Jan. 1993.

4. Barth, T. J.: Numerical Aspects of Computing Viscous High Reynolds Number Flows on Unstructured Meshes. AIAA 29th Aerospace Sciences Meeting, Reno, Nev., Jan. 1991.

5. Stremel, P. M.: The Effect of Upper Surface and Lower surface Fences on Airfoil Aerodynamics at –90 Degrees Incidence. American Helicopter Society Aeromechanics Specialists Conference, San Francisco, Calif., Jan. 19–21, 1994.

6. Hildebrand, F. B.: Advanced Calculus for Applications. Prentice Hall, second edition.

7. Roach, P. J.: Computational Fluid Dynamics. Hermosa Publishers, LCCC# 72-89970.

8. Oswald, G. A.; Ghia, K. N.; and Ghia, U.: A Direct Algorithm for Solution of Incompressible Three-Dimensional Unsteady Navier–Stokes Equations. AIAA Paper 87-1139, Reno, Nev., 1987.

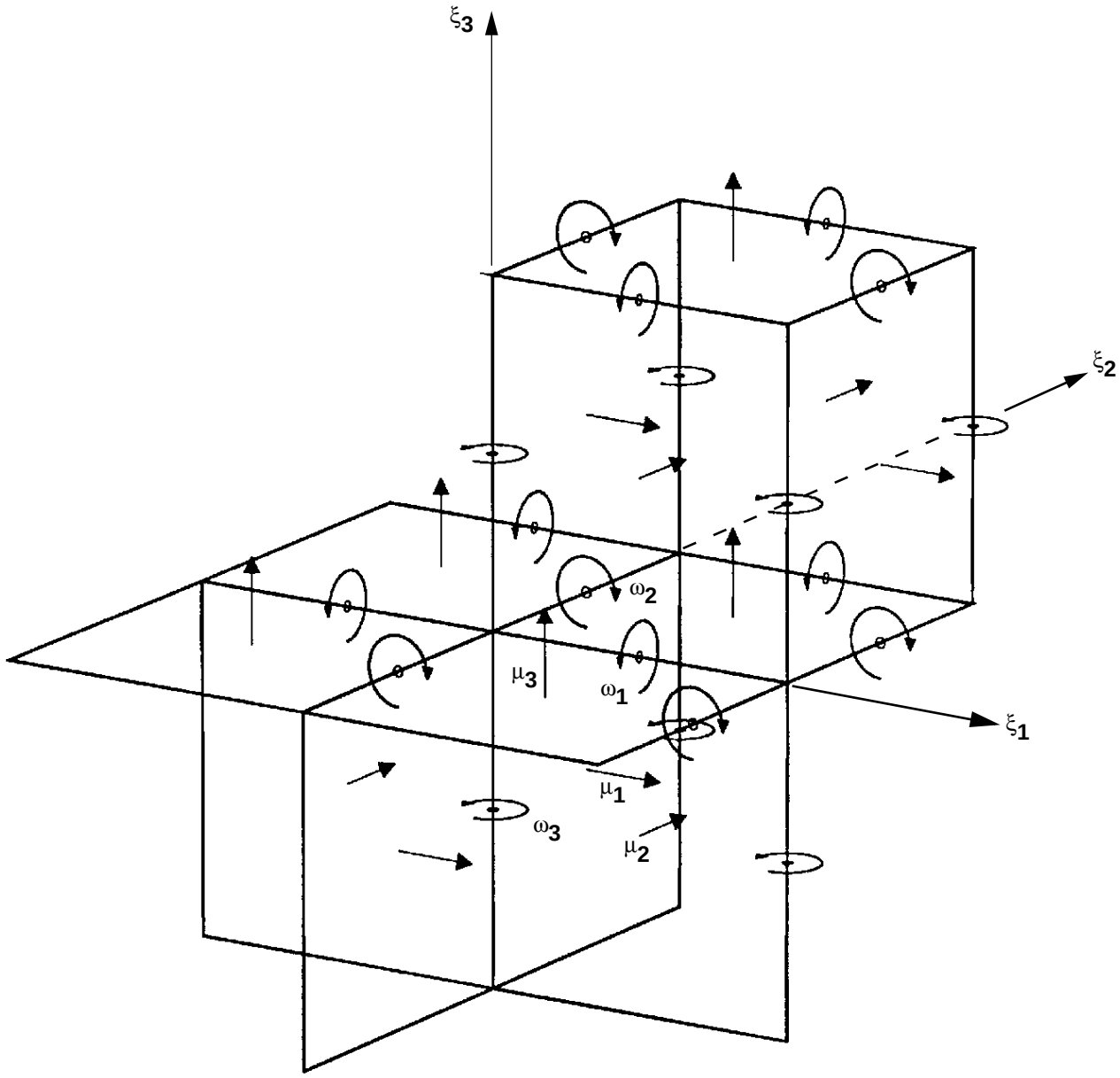

Figure 1. Schematic for staggered-grid formulation.

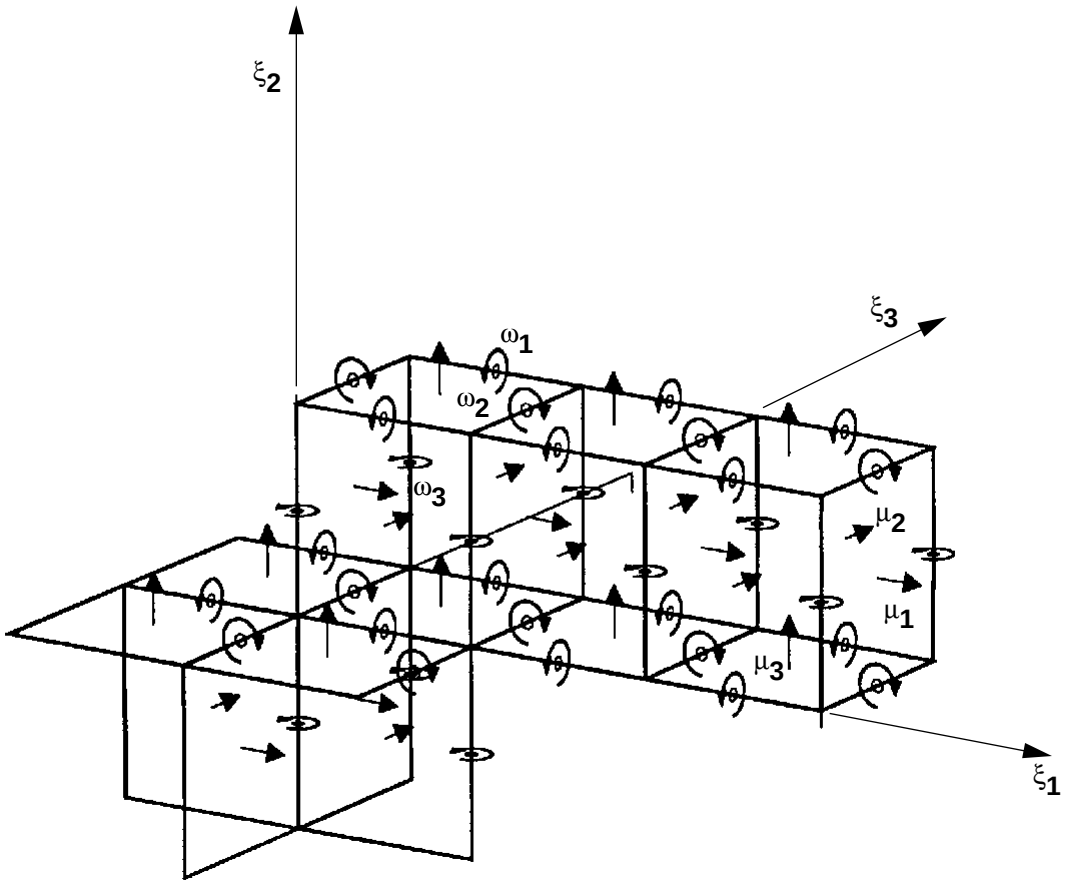

Figure 2. Schematic for staggered-grid formulation, ξ_1 solution sweep.

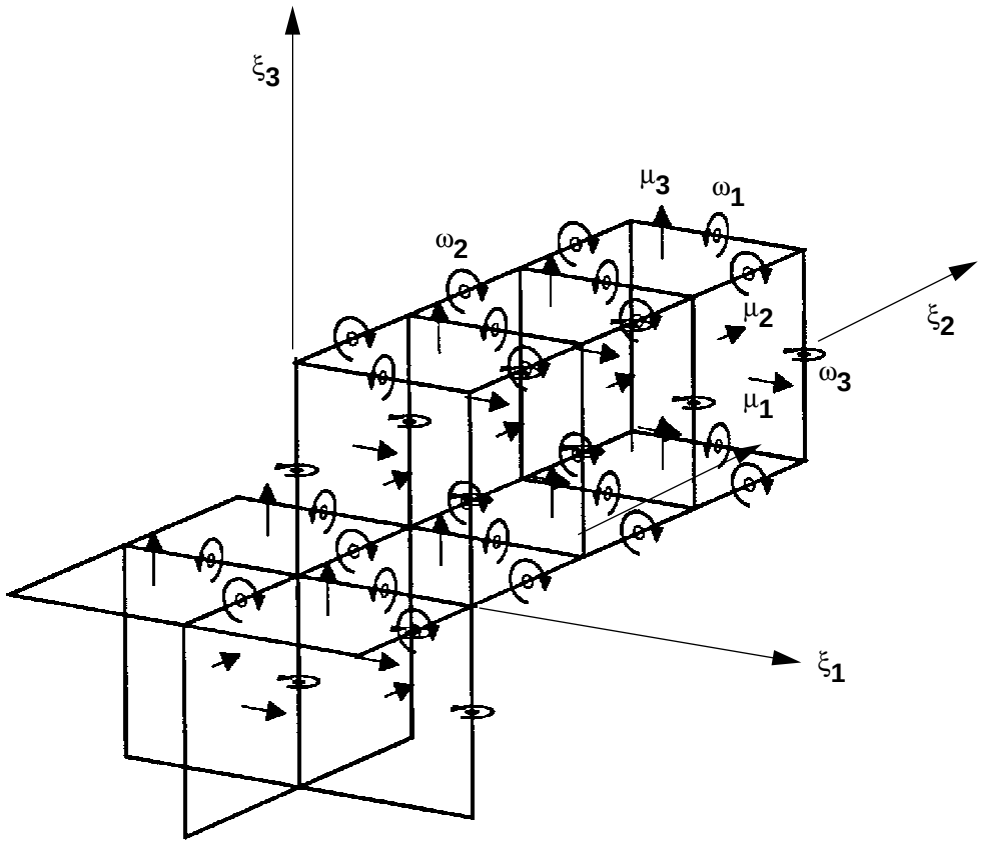

Figure 3. Schematic for staggered-grid formulation, ξ_2 solution sweep.

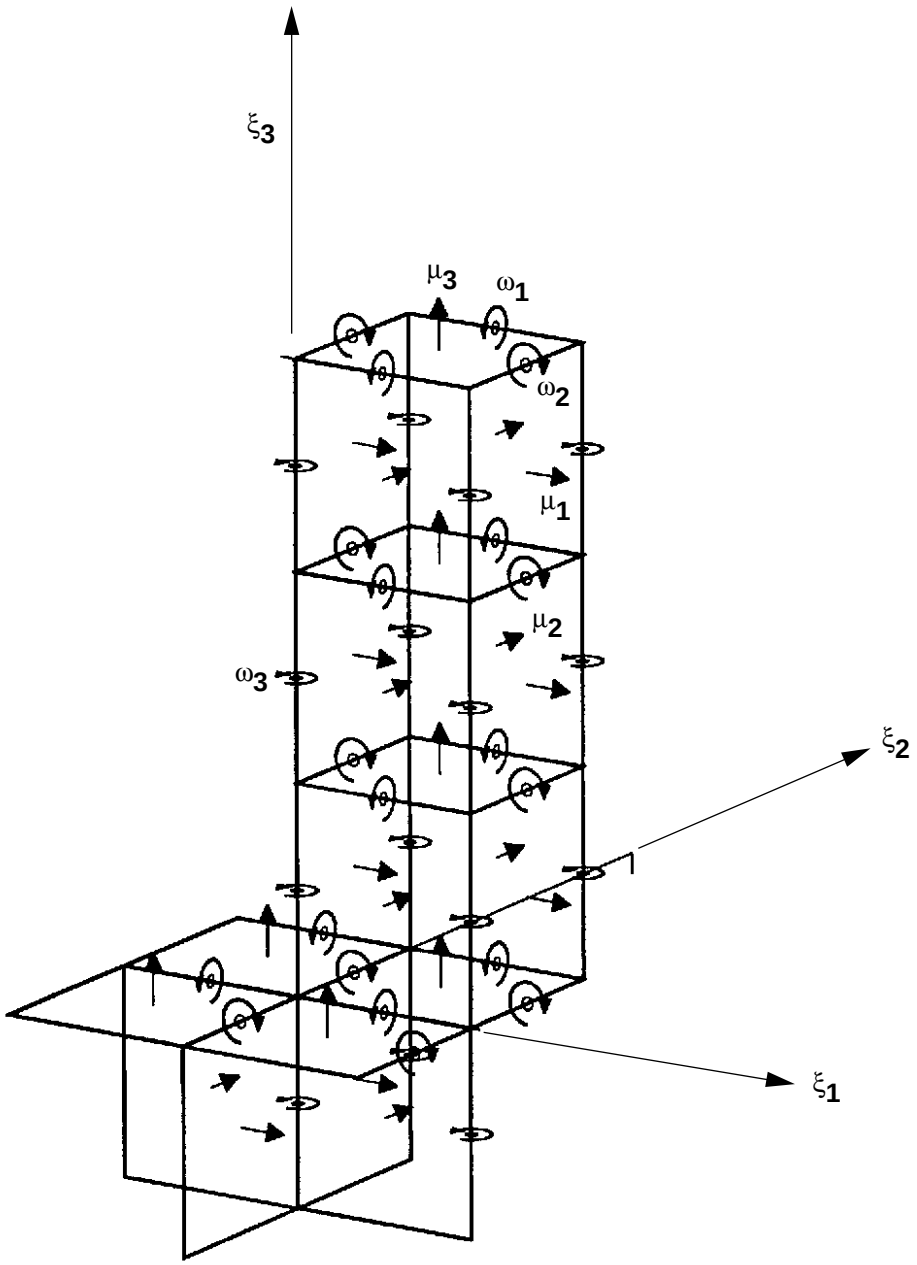

Figure 4. Schematic for staggered-grid formulation, ξ_3 solution sweep.

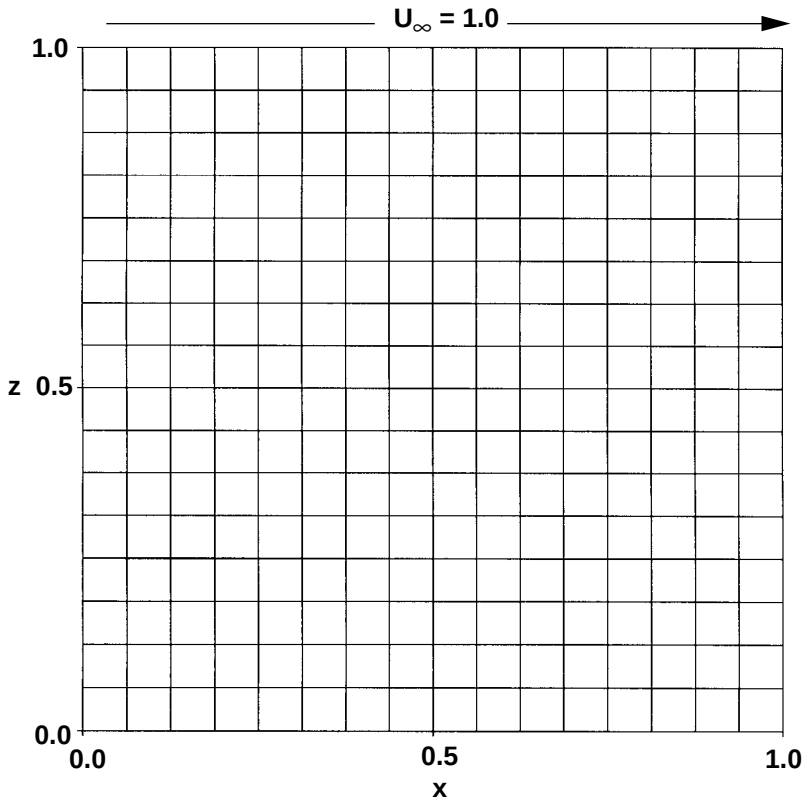

Figure 5. Geometry for cubic cavity, constant spacing, $17 \times 17 \times 17$.

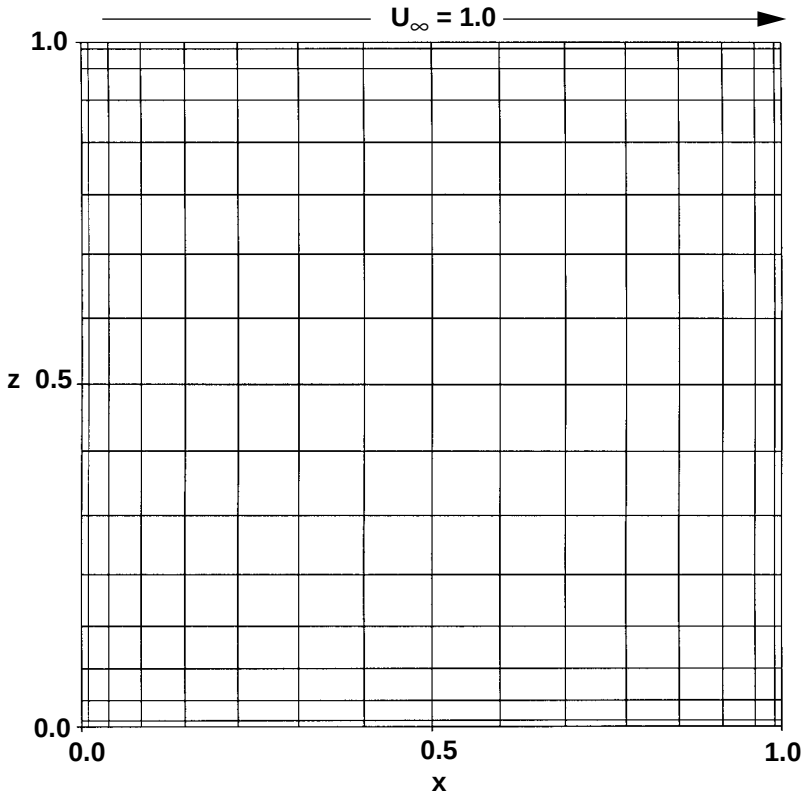

Figure 6. Geometry for cubic cavity, cosine spacing, $17 \times 17 \times 17$.

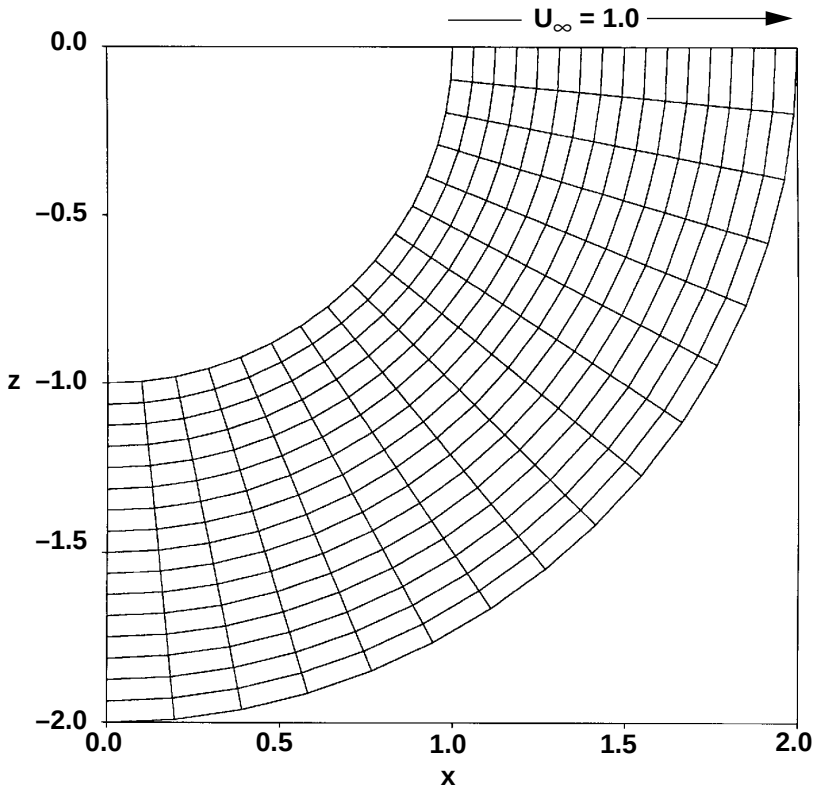

Figure 7. Geometry for curved cavity, constant spacing, $17 \times 17 \times 17$.

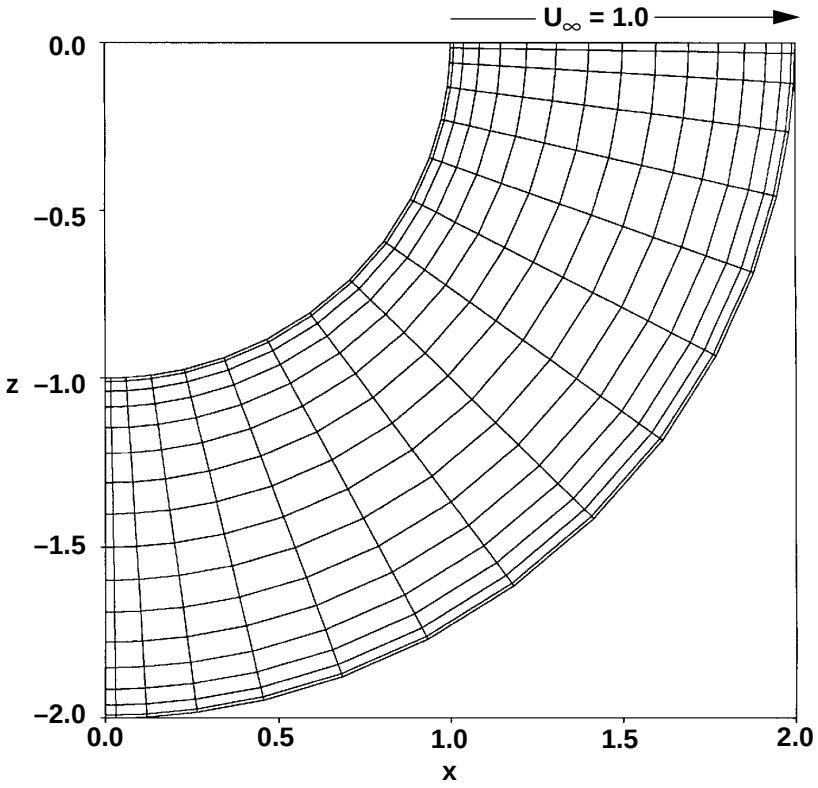

Figure 8. Geometry for curved cavity, cosine spacing, $17 \times 17 \times 17$.

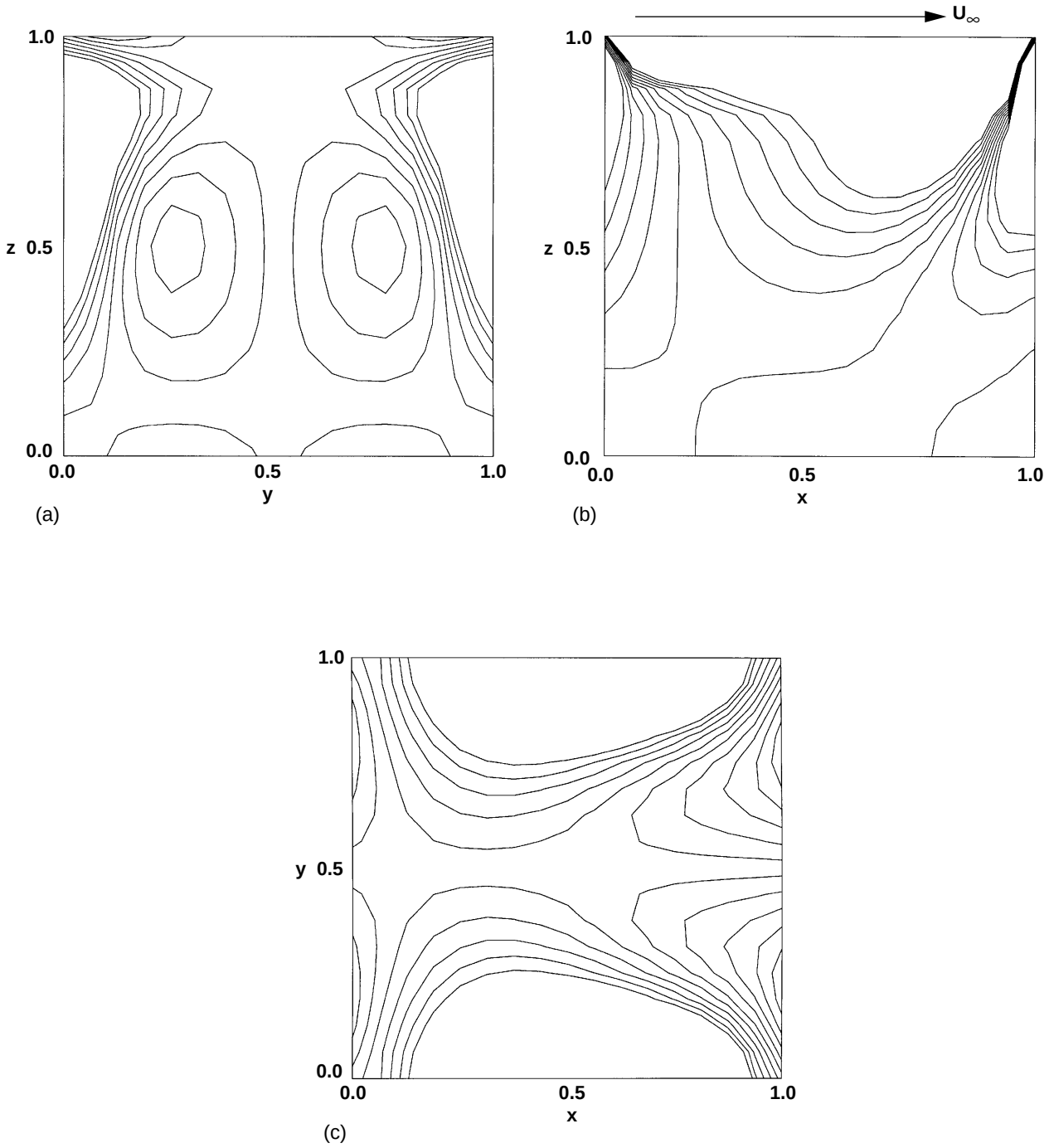

Figure 9. Vorticity contours for cubic cavity, constant spacing, mid-plane locations, $17 \times 17 \times 17$. a) ξ_1 vorticity contours, b) ξ_2 vorticity contours, c) ξ_3 vorticity contours.

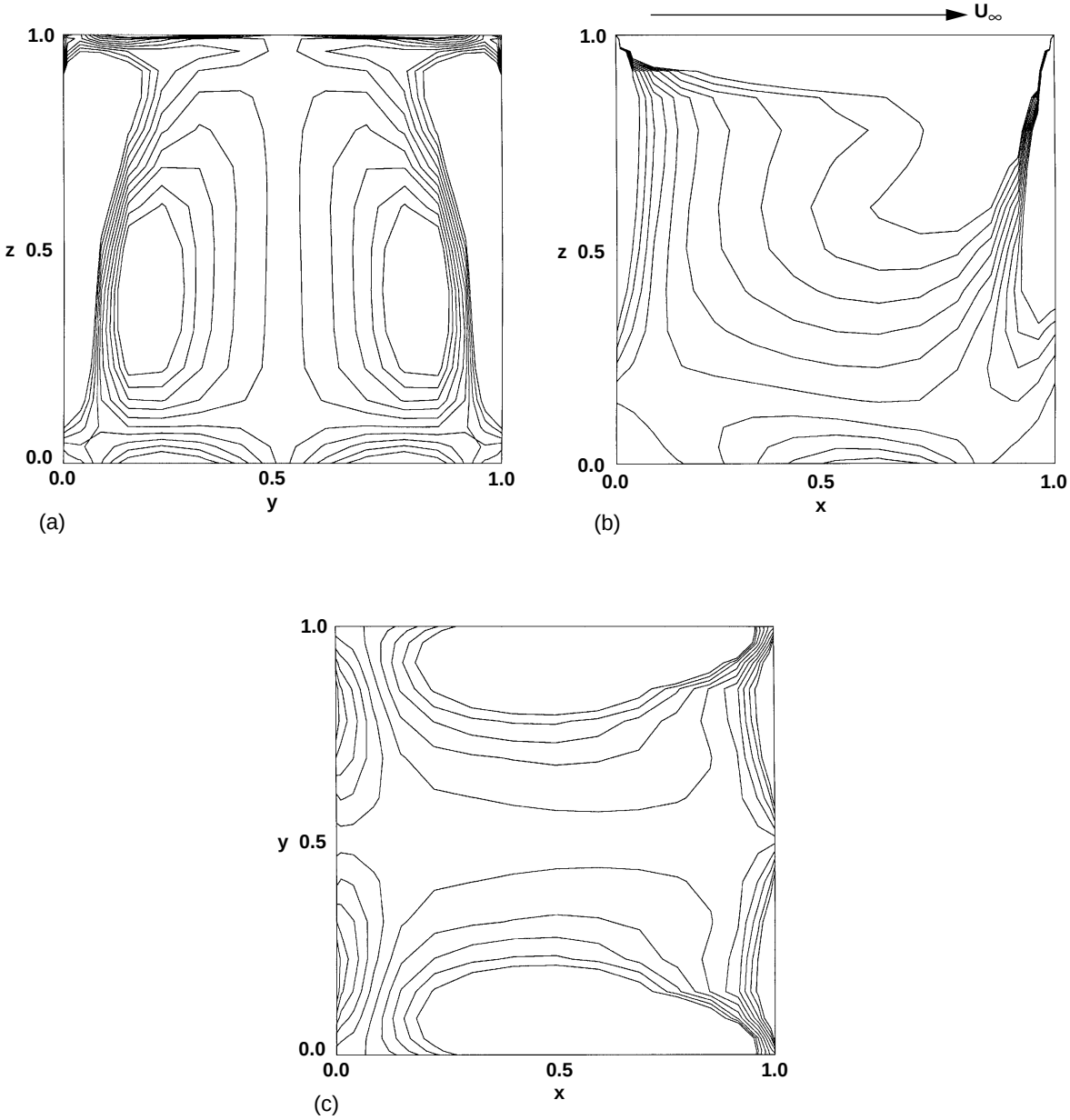

Figure 10. Vorticity contours for cubic cavity, cosine spacing, mid-plane locations, $17 \times 17 \times 17$. a) ξ_1 vorticity contours, b) ξ_2 vorticity contours, c) ξ_3 vorticity contours.

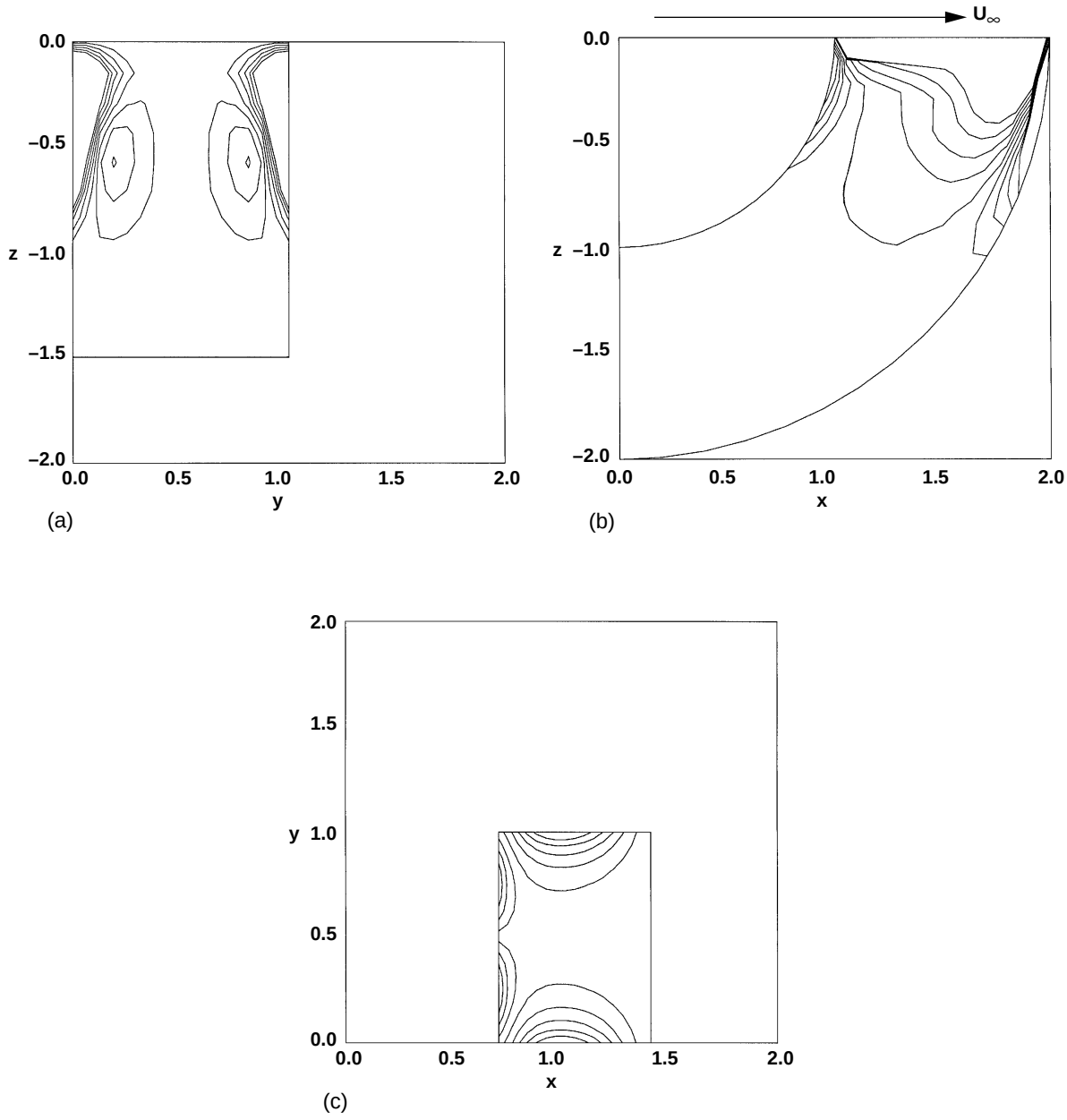

Figure 11. Vorticity contours for curved cavity, constant spacing, mid-plane locations, $17 \times 17 \times 17$. a) ξ_1 vorticity contours, b) ξ_2 vorticity contours, c) ξ_3 vorticity contours.

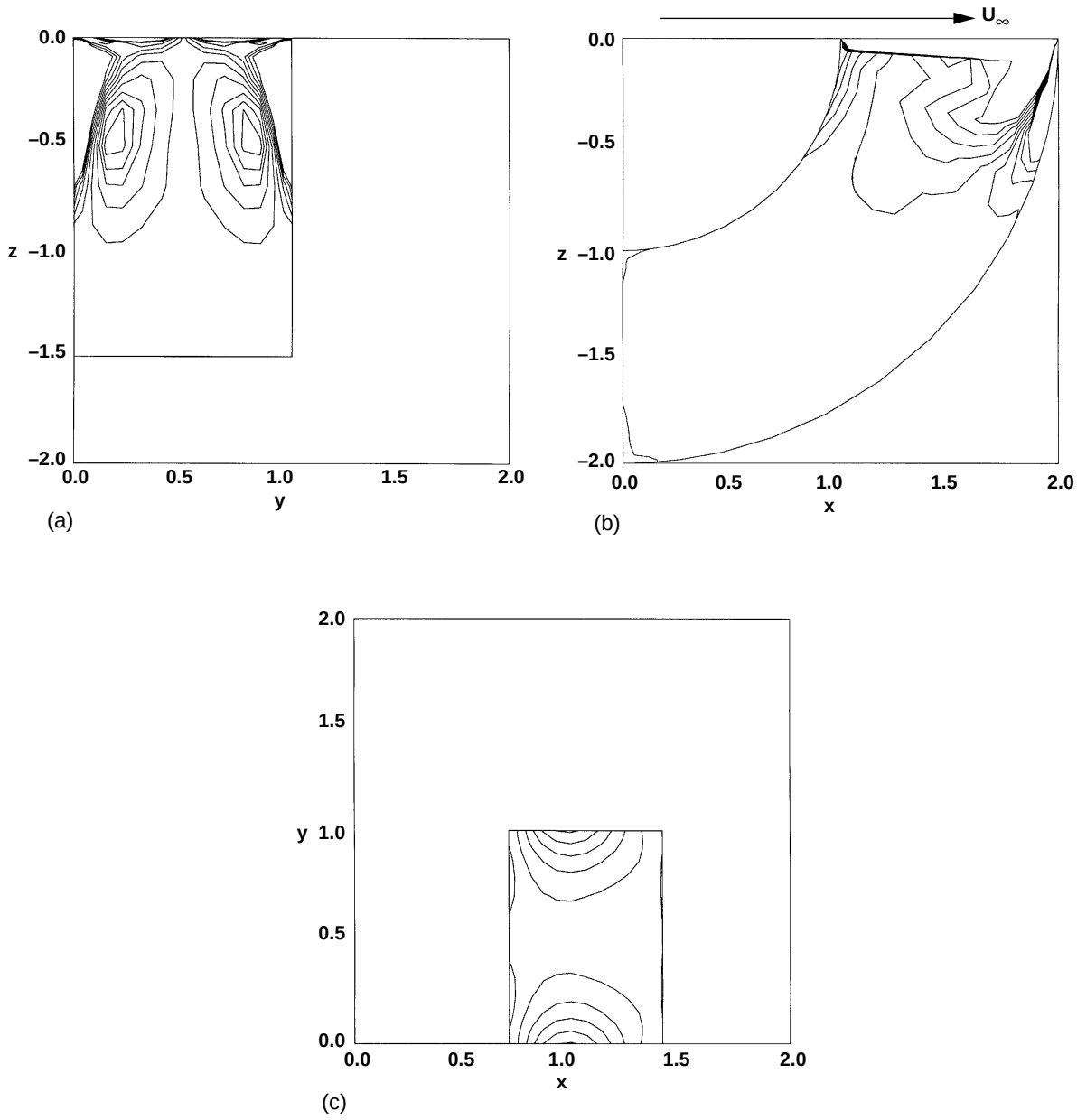

Figure 12. Vorticity contours for curved cavity, cosine spacing, mid-plane locations, $17 \times 17 \times 17$. a) ξ_1 vorticity contours, b) ξ_2 vorticity contours, c) ξ_3 vorticity contours.

REPORT DOCUMENTATION PAGE

Form Approved
OMB No. 0704-0188

1. AGENCY USE ONLY (Leave blank)	2. REPORT DATE	3. REPORT TYPE AND DATES COVERED
	May 1995	Technical Memorandum

4. TITLE AND SUBTITLE

Calculation of Three-Dimensional (3-D) Internal Flow by Means of the Velocity-Vorticity Formulation on a Staggered Grid

5. FUNDING NUMBERS

505-59-36

6. AUTHOR(S)

Paul M. Stremel

7. PERFORMING ORGANIZATION NAME(S) AND ADDRESS(ES)

Ames Research Center
Moffett Field, CA 94035-1000

8. PERFORMING ORGANIZATION REPORT NUMBER

A-950063

9. SPONSORING/MONITORING AGENCY NAME(S) AND ADDRESS(ES)

National Aeronautics and Space Administration
Washington, DC 20546-0001

10. SPONSORING/MONITORING AGENCY REPORT NUMBER

NASA TM-110352

11. SUPPLEMENTARY NOTES

Point of Contact: Paul M. Stremel, Ames Research Center, MS T12-B, Moffett Field, CA 94035-1000
(415) 604-4563

12a. DISTRIBUTION/AVAILABILITY STATEMENT

Unclassified-Unlimited
Subject Category – 02

12b. DISTRIBUTION CODE

13. ABSTRACT (Maximum 200 words)

A method has been developed to accurately compute the viscous flow in three-dimensional (3-D) enclosures. This method is the 3-D extension of a two-dimensional (2-D) method developed for the calculation of flow over airfoils. The 2-D method has been tested extensively and has been shown to accurately reproduce experimental results. As in the 2-D method, the 3-D method provides for the non-iterative solution of the incompressible Navier–Stokes equations by means of a fully coupled implicit technique. The solution is calculated on a body fitted computational mesh incorporating a staggered grid methodology. In the staggered grid method, the three components of vorticity are defined at the centers of the computational cell sides, while the velocity components are defined as normal vectors at the centers of the computational cell faces. The staggered grid orientation provides for the accurate definition of the vorticity components at the vorticity locations, the divergence of vorticity at the mesh cell nodes and the conservation of mass at the mesh cell centers. The solution is obtained by utilizing a fractional step solution technique in the three coordinate directions. The boundary conditions for the vorticity and velocity are calculated implicitly as part of the solution. The method provides for the non-iterative solution of the flow field and satisfies the conservation of mass and divergence of vorticity to machine zero at each time step. To test the method, the calculation of simple driven cavity flows have been computed. The driven cavity flow is defined as the flow in an enclosure driven by a moving upper plate at the top of the enclosure. To demonstrate the ability of the method to predict the flow in arbitrary cavities, results will be shown for both cubic and curved cavities.

14. SUBJECT TERMS

Velocity, Vorticity, Driven cavity

15. NUMBER OF PAGES

35

16. PRICE CODE

A03

17. SECURITY CLASSIFICATION OF REPORT	18. SECURITY CLASSIFICATION OF THIS PAGE	19. SECURITY CLASSIFICATION OF ABSTRACT	20. LIMITATION OF ABSTRACT
Unclassified	Unclassified		